Human Pathology (2019) **83**, 22–28

ELSEVIER

Human PATHOLOGY

www.elsevier.com/locate/humpath

Original contribution

Expressions of ATF6, XBP1, and GRP78 in normal tissue, atypical adenomatous hyperplasia, and adenocarcinoma of the lung☆,☆☆

Sho Ogata MD[a,*], Koji Kameda MD[a,b], Takako Kono MD[c], Yuichi Ozeki MD[b], Hiroshi Hashimoto MD[b], Susumu Tominaga MT[a], Kuniaki Nakanishi MD[a]

[a]*Department of Pathology and Laboratory Medicine, National Defense Medical College, Tokorozawa, Saitama 359-8513, Japan*
[b]*Department of Surgery, National Defense Medical College, Tokorozawa, Saitama 359-8513, Japan*
[c]*Department of Pathology, National Defense Medical College, Tokorozawa, Saitama 359-8513, Japan*

Received 1 June 2018; revised 9 August 2018; accepted 12 August 2018

Keywords:
Atypical adenomatous hyperplasia;
Pulmonary adenocarcinoma in situ;
ER stress;
ATF-6;
XBP1;
GRP78

Summary Little is known about the association between the atypical adenomatous hyperplasia (AAH)–adenocarcinoma in situ sequence of the lung and endoplasmic reticulum–stress responders such as ATF6, XBP1, and GRP78. Using stored tissues, we examined (i) the percentage of a splicing form (active form) of *XBP1* messenger RNA in normal lung tissue (NLT) and adenocarcinoma (ACA; using reverse-transcription polymerase chain reaction); (ii) ATF6 and GRP78 protein expressions in NLT and ACA (using Western blotting analysis); (iii) ATF6, XBP1, and GRP78 protein expressions in NLT, AAH, and ACA, including some adenocarcinoma in situ (using immunohistochemistry); and (iv) the incidence of nuclear translocation of the 3 proteins in these lesions. The percentage of the splicing form of *XBP1* messenger RNA showed a borderline difference between NLT and ACA ($P = .068$). In the Western blotting analysis, the nuclear fractions of ATF6 (including the active form) and GRP78 proteins were higher in ACA than in NLT. In the immunohistochemistry, the values obtained for the incidence of the nuclear translocation of ATF6, XBP1, and GRP78 proteins were as follows, respectively: 13.3%, 2.2%, and 0.5% in low-grade AAH; 37.9%, 2.3%, and 2.2% in high-grade AAH; and 47.2%, 10.6%, and 4.4% in ACA. A significant difference was detected between low-grade AAH and ACA for ATF6. In terms of nuclear translocation, high-grade AAH seemed intermediate between low-grade AAH and ACA. These results support endoplasmic reticulum–stress responses, such as nuclear translocation of these 3 proteins (including their active forms), being in parallel with the progression of the adenoma-carcinoma sequence in the lung.

1. Introduction

Atypical adenomatous hyperplasia (AAH) of the lung is a proliferation of type II alveolar pneumocytes and/or Clara cells. Although adenocarcinoma in situ (AIS) of the lung is defined as an adenocarcinoma (ACA) with a pure lepidic growth pattern and no evidence of stromal, vascular, or pleural

☆ Competing interests: None declared.
☆☆ Funding/Support: This study was supported by grants from the Ministry of Defense of Japan.
* Corresponding author at: Department of Pathology and Laboratory Medicine, National Defense Medical College, 3-2 Namiki, Tokorozawa 359-8513, Japan.
E-mail address: sogata@ndmc.ac.jp (S. Ogata).

https://doi.org/10.1016/j.humpath.2018.08.009
0046-8177/

invasion, neither its histogenesis nor the relationship between AAH and AIS is well understood [1-3].

The endoplasmic reticulum (ER) is an important cell organelle that is responsible for the correct folding and sorting of proteins [4]. The functions of the ER are disturbed when unfolded or misfolded proteins accumulate within it (termed "ER stress") [4,5]. ER stress is linked to neurodegenerative diseases such as Parkinson and Alzheimer diseases [6-10] and triggers the unfolded protein response (UPR), which improves cell survival by limiting ER stress [11,12]. UPR is initiated through signaling by ER-localized transmembrane proteins, such as ER stress response factor, a heterogeneous protein complex [13,14]. Activating transcription factor-6 (ATF6) and X-box binding protein 1 (XBP1) are inducible components of ER stress response factor [15,16]. ATF6, a 670-amino-acid glycoprotein with the electrophoretic mobility of a 90-kDa protein (p90ATF6), is an ER membrane-bound transcription factor. ER stress induces proteolysis of membrane-bound p90ATF6, releasing the N-terminal half of the active form, p50ATF6, which is then translocated into the nucleus. Concerning XBP1, transcription of *XBP1* messenger RNA (mRNA) is induced by ATF6, and it is spliced by an ER-resident protein kinase and endonuclease, inositol-requiring enzyme 1 (IRE1), resulting in the production of an active transcription factor (pXBP1[S]), and this is then translocated into the nucleus [16]. Both p50ATF6 and pXBP1(S) can bind to ER stress response elements and induce transcription of ER chaperon genes [17,18]. Furthermore, activations of ATF6 and XBP1 are controlled by the chaperone 78-kDa glucose-regulating protein (GRP78), which is localized to the ER [16,17]. GRP78 acts as a central regulator of ER homeostasis, and its up-regulation is widely used as a sentinel marker for ER stress under pathologic conditions [19]. In addition to its ER localization, GRP78 protein has recently been found to be localized on the cell surface, as well as in the mitochondrion and nucleus, and beyond the ER, the mitochondrial and nuclear forms of GRP78 have been suggested to be linked to cellular homeostasis [19].

The importance of ER stress and UPR in carcinogenesis and for the prognosis of several cancers, including lung cancer, has been widely studied [4,5,19-24], and in the future, important roles may be found for therapies targeting this pathway. In the lung, GRP78 expression has been shown to be significantly higher in invasive ACAs than in AAH [24], but little is known about the role of ER stress responses in the adenoma-carcinoma sequence [20-22,24]. We therefore investigated (i) whether a splicing form (active form) of *XBP1* mRNA might be expressed in normal lung tissues (NLTs) and/or in the present ACAs; (ii) whether ATF6 and GRP78 proteins might be distributed in the cytosol and/or nucleus of cells in NLTs and/or the present ACAs; (iii) whether different distributions of ATF6, XBP1, and GRP78 proteins would be revealed among the 3 lesions (low- and high-grade AAH and ACA); and (iv) whether the incidence with which expressions of the active forms of ATF6 and XBP1 proteins and GRP protein are translocated to the nucleus might differ among the above 3 lesions.

2. Materials and methods

From 1980 to 2002, the surgical pathology services of the National Defense Medical College Hospital, Tokorozawa, received fresh-frozen tissues from 23 NLTs (resected from 23 patients with lung cancer) and 30 ACAs (resected from 30 patients and comprising 29 nonmucinous ACAs at least focally with lepidic growth and 1 AIS, each of which measured ≤30 mm in greatest diameter), and also formalin-fixed, paraffin-embedded specimens of 35 AAH lesions of the lung (resected from 18 patients) and 34 ACAs (resected from 34 patients and comprising 25 nonmucinous ACAs at least focally with lepidic growth and 9 AIS, each measuring ≤20 mm in greatest diameter). For 7 of the 18 patients with AAH, the specimens were stock materials of unknown origin. Of the 35 AAH lesions, 15 were interpreted as high grade on the basis of the finding of increased cellularity and cytologic pleomorphism [25-27].

2.1. Reverse-transcription polymerase chain reaction

Total mRNAs were obtained from the fresh-frozen specimens of the 23 NLTs and 30 ACAs that were available to us. Total RNA was isolated using acid guanidinium isothiocyanate–phenol–chloroform extraction and ethanol precipitation. Reverse-transcription polymerase chain reaction (RT-PCR) was performed using a reverse transcription reagent kit (high-capacity cDNA kit; Applied Biosystems, Alameda, CA) and an amplification reagent kit (TaqMan EZRT-PCR kit; Applied Biosystems) as previously reported [25]. The sense and antisense sequences of the *XBP1* primers were 5′-CCA GTG GCC GGG TCT G-3′ and 5′-CAG AAT GCC CAA CAG GAT ATC A-3′, respectively. PCR products were separated by electrophoresis in a 3% to 4% agarose gel or 10% SDS-PAGE gel and then stained with ethidium bromide. The ratio of relative scan units for *XBP1* mRNA on the membrane was calculated as follows: spliced form over unspliced form plus spliced form.

2.2. Western blotting analysis

The nuclear and cytosolic fractions from 2 paired tissues (NLT and ACA from the same patient) were isolated using a nuclear/cytosol fractionation kit (Biovision Research Products, Mountain View, CA). Protein concentration was quantified using a DC Protein Assay kit (Bio-Rad). Equal amounts of nuclear and cytosolic protein extracts were separated by 7.5% SDS-PAGE and transferred to polyvinylidene difluoride membranes (Hybond-N+; Amersham Pharmacia Biotech, Buckinghamshire, England). The membranes were blocked with 5% nonfat dry milk for 60 minutes at room temperature and then incubated overnight at 4°C with primary antibodies against ATF6 (5 μg/mL; clone No. 70B1413; Imgenex, San Diego, CA) and GRP78 (1:10; Thermo Scientific Pierce Antibodies, Fremont, CA). Then, blots were incubated for 1 hour with horseradish peroxidase–conjugated secondary antibodies

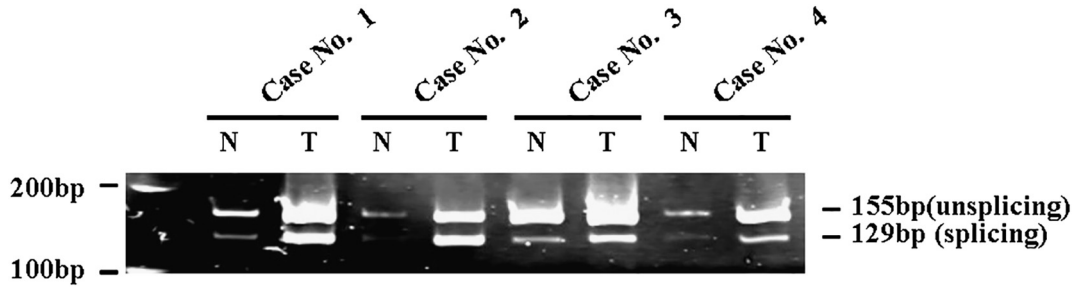

Fig. 1 Semiquantitative RT-PCR for *XBP1* mRNA in NLTs (N) and ACAs (T). PCR products were detected at 155 bp (unspliced form) and 129 bp (spliced form) in NLTs and ACA tissues in these 4 patients (case numbers: 1-4).

and visualized by enhanced chemiluminescence (Amersham Life Science, Arlington Heights, IL).

2.3. Immunohistochemistry

The polymer-peroxidase method (EnVision+/HRP; Dako Cytomation, Glostrup, Denmark) was applied to deparaffinized sections of 35 AAHs and 34 ACAs using mouse monoclonal antibodies against ATF6 (1:100; clone No. 70B1413; Imgenex) and rabbit polyclonal antibodies against XBP1 (1:40; Santa Cruz Biotechnology, Santa Cruz, CA) and GRP78 (ready-to-use; Thermo Scientific Pierce Antibodies). For XBP1, the sections were boiled in 0.01 M Tris–0.001 M EDTA buffer (pH 9.0) for 60 minutes before immunohistochemistry (IHC) against the antibody. For the negative control, the incubation step with the primary antibody was omitted.

For the analysis of cytoplasmic staining, the intensity and extent of staining were scored from 0 to 3 and from 0 to 4, respectively, with 0 representing no staining. The intensity was scored as 1 indicating weak, 2 indicating moderate, and 3 indicating strong staining. The extent of staining was scored as follows: 0, indicating negative reaction of tumor cells; 1, 10% or less of tumor area stained; 2, 11% to 25% stained; 3, 26% to 50% stained; or 4, at least 51% stained. For the analysis of nuclear staining of ATF6, XBP1, and GRP78, the percentage of nuclei exhibiting a positive immunoreaction was determined on the basis of the immunoreaction in at least 500 cells of AAH and in at least 1000 cells of ACA, in each case within the area of greatest immunoreaction.

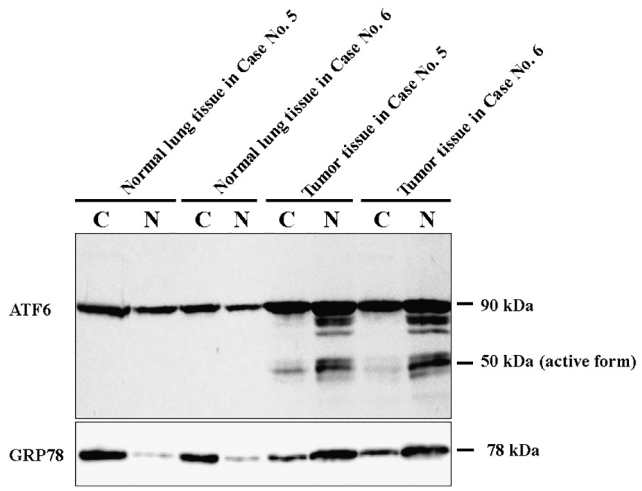

Fig. 2 Western blotting analyses of ATF6 and GRP78 proteins in cytoplasmic (C) and nuclear (N) fractions in NLTs and ACAs. Both ATF6 and GRP78 proteins were detected in both fractions in normal lung and tumor (ACA) tissues from these 2 patients (case numbers: 5 and 6). In contrast to the findings in normal tissue, in tumor tissue, the active form (50 kDa) of ATF6 protein was exhibited by the cytoplasmic and nuclear fractions (predominantly by the nuclear fraction) and expression of GRP78 protein was detected predominantly in the nuclear fraction.

2.4. Ethics and data analysis

The present study was approved by the institutional review board in the National Defense Medical College (No. 2812; January 9, 2018). Differences between 2 groups in the ratio of relative scan units (spliced form over unspliced form plus spliced form) for *XBP1* mRNA were analyzed statistically using an unpaired Student *t* test. For the percentage of nuclear expressions of ATF6, XBP1, and GRP78 proteins (by IHC), Scheffe test was applied to the data when significant *F* ratios were obtained in an analysis of variance. For the cytoplasmic expressions of the above 3 proteins, the Kruskal-Wallis test was performed. A *P* value less than .05 was considered significant.

3. Results

3.1. Clinicopathological findings in AAH

There were 18 patients with a total of 35 AAH lesions. For 4 of these 18 patients, age and sex were uncertain. Ten of the remaining 14 patients were male. Age at diagnosis was within the range 51 to 71 years, with a median age of 62 years. Among the 18 cases with 35 AAH lesions, 13 cases had only 1 AAH lesion. Five of these 18 cases were without lung cancer. Among the 13 cases that did have lung cancer, there were 12 cases of ACA and 1 of large cell carcinoma. The median diameter of the AAH lesions was 2 mm (range, 1-13 mm). In terms of diameter, there was no significant difference between

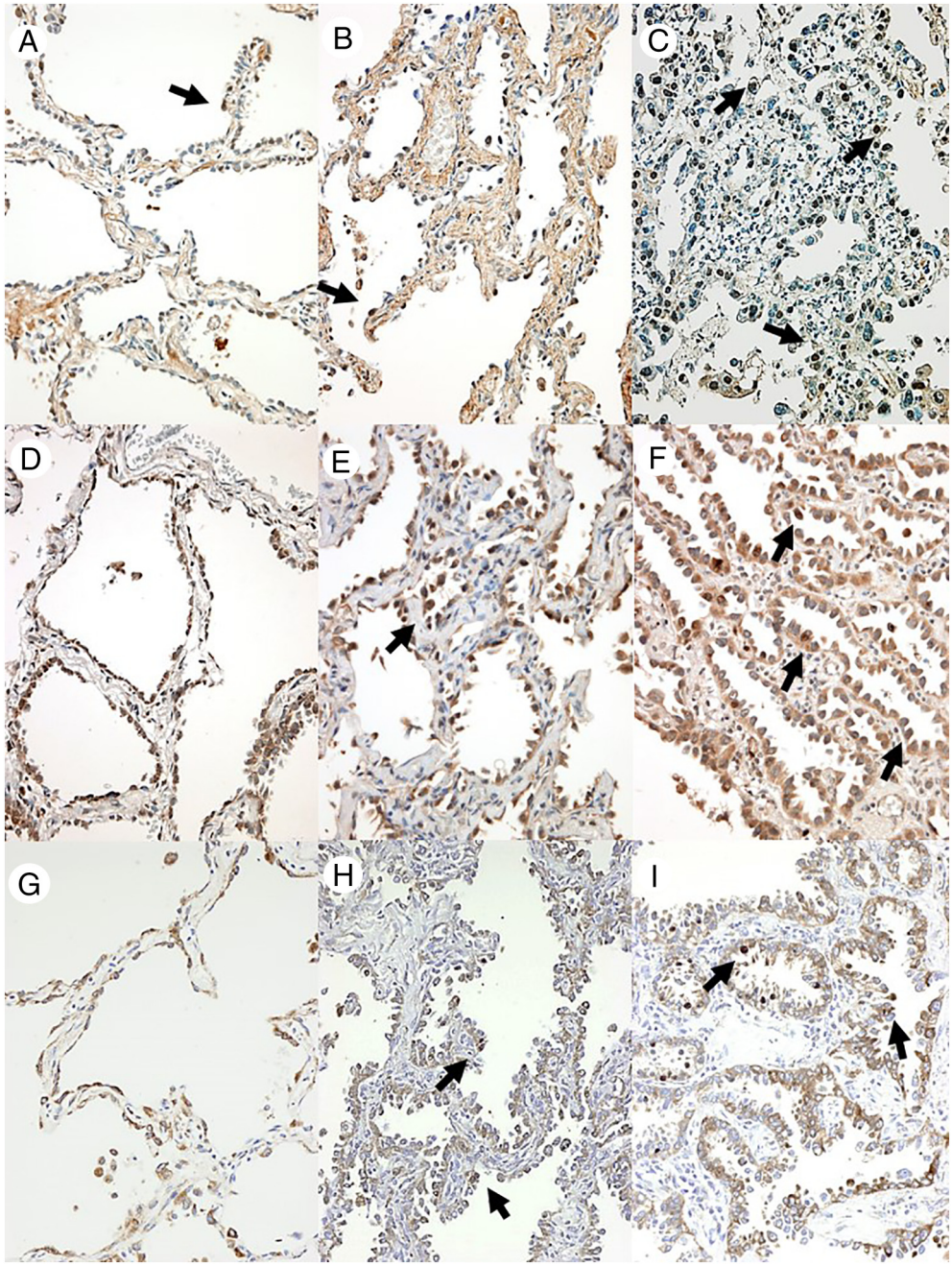

Fig. 3 Immunohistochemical expressions of ATF6, XBP1, and GRP78 proteins in AAH and ACA. ATF-6 (A-C), XBP1 (D-F), and GRP78 (G-I) were expressed in the cytoplasm and nuclei (arrows) of AAH (low-grade [A, D, and G), high-grade [B, E, and H]) and ACA (C, F, and I). Scale bars, 100 μm.

low-grade AAH lesions (mean ± SD, 2.3 ± 2.4 mm) and high-grade AAH lesions (4.1 ± 3.2 mm). Of the 35 AAH lesions, 15 were interpreted as high grade on the basis of the finding of increased cellularity and cytologic pleomorphism [25,26].

3.2. RT-PCR for *XBP1* mRNA in NLTs and ACAs

PCR products for *XBP1* mRNA were detected at 155 bp (unspliced form) and 129 bp (spliced form) in NLTs and ACAs (Fig. 1). The mean ± SD for the ratio of relative scan units for *XBP1* mRNA (spliced form over unspliced form plus spliced form) was 3.8% ± 5.0% in the 23 NLTs and 6.8% ± 7.2% in the 30 ACAs (borderline difference, $P = .068$).

3.3. Western blotting analyses of ATF6 and GRP78 proteins in NLTs and ACAs

ATF6 and GRP78 proteins were detected in the cytoplasmic and nuclear fractions both in NLTs and in ACAs (Fig. 2). The active form (50 kDa) of ATF6 protein was

Table Immunohistochemical expressions of ATF6, XBP1, and GRP78 proteins in AAH and nonmucinous ACA of the lung

	No. of lesions	Nuclear labeling index (%) [a]	Cytoplasmic IHC score [b]
ATF6			
AAH			
Total	35	23.8 ± 19.4 [c]	0.2 ± 1.0
Low-grade	20	13.3 ± 10.7 *,***	0.1 ± 0.4 ***
High-grade	15	37.9 ± 19.6 *	0.4 ± 1.5 ***
ACA	34	47.2 ± 23.9 **	2.2 ± 2.3 ***
XBP1			
AAH			
Total	35	2.3 ± 2.7	3.0 ± 2.6
Low-grade	20	2.2 ± 2.7	2.6 ± 2.5 ****
High-grade	15	2.3 ± 2.9	3.5 ± 2.7 ****
ACA	34	10.6 ± 17.9	4.8 ± 2.1 ****
GRP78			
AAH			
Total	34	1.2 ± 2.1	5.3 ± 0.3
Low-grade	19	0.5 ± 0.5	5.1 ± 2.3
High-grade	15	2.2 ± 2.9	5.2 ± 1.7
ACA	33	4.4 ± 8.3	4.6 ± 1.8

[a] For the analysis of nuclear staining of ATF6, XBP1, and GRP78, the percentage of nuclei exhibiting a positive immunoreaction was determined on the basis of the immunoreaction in at least 500 cells of AAH and in at least 1000 cells of ACA, in each case within the area of greatest immunoreaction. For statistical analysis, Scheffe test was applied to the data when significant *F* ratios were obtained in an analysis of variance.

[b] For the analysis of cytoplasmic IHC staining, the intensity and extent of staining were scored from 0 to 3 and from 0 to 4, respectively, with 0 representing no staining. The intensity was scored as 1 indicating weak, 2 indicating moderate, and 3 indicating strong staining. The extent of staining was scored as follows: 0, indicating negative reaction of tumor cells; 1, 10% or less of tumor area stained; 2, 11% to 25% stained; 3, 26% to 50% stained; or 4, at least 51% stained. For statistical analysis, the Kruskal-Wallis test was performed.

[c] Mean ± SD.

* $P = .0027$.

** $P < .0001$.

*** $P = .0033$.

**** $P = .0033$.

detected in the cytoplasmic and nuclear fractions in ACAs, predominantly in the nuclear fraction, but it was not detected at all in NLTs. GRP78 protein in NLT was higher in the cytoplasmic fraction than in the nuclear fraction, whereas it was detected predominantly in the nuclear fraction in ACA.

3.4. Distributions of ATF6, XBP1, and GRP78 proteins in NLTs by IHC

By IHC, ATF6 protein was found to be either not stained at all or only very weakly stained in the cytoplasm of a variety of lung components, with sometimes weak staining in the nucleus of bronchial surface epithelial cells (data not shown). The expressions of XBP1 and GRP78 proteins seemed weak and diffuse in the cytoplasm of cells within NLT, such as bronchial surface epithelial cells, chondrocytes of the bronchial cartilage, serous cells of the bronchial glands, and alveolar macrophages. XBP1 and GRP78 proteins were almost never detected in the nucleus (data not shown).

3.5. IHC expressions of ATF6, XBP1, and GRP78 proteins in AAHs and ACAs

Expressions of ATF6, XBP1, and GRP78 proteins were confined to the cytoplasm and nuclei of hyperplastic and neoplastic cells (Fig. 3). For a given protein, the intensity of staining sometimes varied within a given case.

Concerning the cytoplasmic expression, the mean IHC score for ATF6 protein and that for XBP1 protein increased significantly along the progression from low-grade AAH through high-grade AAH to ACA ($P < .05$). However, the mean IHC score for GRP78 protein did not differ among the 3 lesions (Table).

Concerning nuclear expression, the mean positive percentage for ATF6, XBP1, and GRP78 proteins increased progressively from low-grade AAH through high-grade AAH to ACA. Statistically, a significant difference for ATF6 protein was demonstrated between low-grade AAH and high-grade AAH, and between low-grade AAH and ACA. However, the mean positive percentages for XBP1 and GRP78 proteins did not differ among the 3 lesions (Table).

4. Discussion

The purpose of our investigation was to seek a better understanding of the relation between the ER stress response and the pathogenesis of peripherally located AIS. We observed that the splicing form of *XBP1* mRNA did not differ statistically between ACAs and NLTs, although there seemed to be borderline significance. In our Western blotting analysis, ATF6 and GRP78 proteins were detected in both cytoplasm and nucleus in NLT and in ACA, and the active form of ATF6 protein, and also GRP78 protein, had evidently translocated from the cytoplasm to the nucleus in ACAs. Furthermore, we found that for AFT6, XBP1, and GRP78 proteins, the percentage of cells with nuclear staining was higher in ACAs than in low-grade AAH or total AAH. In the case of ATF6 and GRP78 proteins, the percentage increased from low-grade AAH to high-grade AAH to ACA (with the positive percentage in high-grade AAH apparently being intermediate between those in low-grade AAH and ACA, and in the case of ATF6 protein tending to be closer to the latter than to the former). Moreover, the cytoplasmic IHC staining score for ATF6 protein and that for XBP1 protein increased significantly from low-grade AAH to high-grade AAH to ACA (Kruskal-Wallis test). Hence, our results are consistent with an up-regulation of the response to ER stress being related to the development of AIS. In the future, application of targeted therapies to this pathway may provide a valuable addition to the currently available strategies.

In the present study, ATF6 was not stained, or stained very weakly, in a variety of lung components. Our Western blotting analysis results revealed ATF6 protein to be represented only by the 90-kDa protein in the cytosolic and nuclear fragments of NLTs. In contrast, by IHC ATF6 protein was sometimes detected in the nucleus in AAH and ACA, whereas the active form of ATF6 (50 kDa) was detected by Western blotting analysis in the nuclear fragment of ACA. However, little or none of the active form was detected in the cytosol fragment of ACA. In our IHC, the number of cells with nuclear expression of ATF6 protein was higher in ACA than in low-grade AAH. It is well known that in several culture cells, ATF6 protein is transformed to its active form under ER stress, and that this active form is then translocated into the nucleus [15,16]. Thus, our results are consistent with a hypothesis in which activation of ATF6 protein occurs during the development of ACA and is in parallel with the progression of the adenoma-carcinoma sequence in the lung. Furthermore, nuclear expression of ATF6 protein may be a useful tool for differential diagnosis of AAH from reactive proliferation. Likewise, in our RT-PCR for *XBP1* mRNA, we found the splicing form in NLTs and ACAs, and the ratio obtained for the splicing form tended to be higher in ACAs than in NLTs. In our IHC for XBP1 protein, the percentage of nuclear-positive tumor cells was higher for ACAs than for either low-grade AAH or total AAH. These findings support a hypothesis for XBP1 protein that is similar to that outlined above for ATF6 protein. Interestingly, in recent reports on breast and lung cancers, an increase in the spliced form of *XBP1* mRNA was found to be associated with poor survival [23,24]. In future, additional studies will be required to examine whether biologic aggressiveness (poor survival, relapse, metastasis) is associated with changed expressions of these proteins.

For GRP78, too, we demonstrated that its protein exhibited translocation to the nucleus in ACA (by Western blotting analysis) and that the percentage of nucleus-positive cells was higher in ACA than in AAH (by IHC). Interestingly, a recent report revealed translocation of GRP78 protein into the nucleus under ER stress and suggested that this might defend against DNA damage–induced apoptosis through a distinct regulatory mechanism within the nucleus [19]. Kim et al [21], who used IHC to examine GRP78 protein in 9 AAHs, 21 bronchioloalveolar carcinomas (ie, AISs), and 56 invasive ACAs, observed significantly lower positivity in AAH than in invasive ACAs and suggested that GRP78 expression is up-regulated during tumor development from the benign or preinvasive stage to the malignant or invasive stage. However, they did not mention nuclear expression of GRP78. We are unsure of the reason for this apparent discrepancy concerning GRP78 cytoplasmic expression between our results and those of Kim et al. One possibility is the use of different materials, and another is the use of different antibodies.

In conclusion, the results of our study of the nuclear translocation of ER stress proteins support a possible involvement of such translocation in the progression of the adenoma-carcinoma sequence in the lung.

Acknowledgment

We wish to thank Dr Robert Timms for correcting the English version of the manuscript.

References

[1] Travis WD, Brambilla E, Burke AP, Marx A, Nicholson G. The WHO Classification of Tumours of Lung, Pleura, Thymus and Heart. 4th edition. Lyon: International Agency of Research on Cancer; 2015. p. 32-50.
[2] Shimosato Y, Kodama T, Kameya T. Morphogenesis of peripheral type adenocarcinoma of the lungs. In: Shimosato Y, Melamed MR, Nettesheim P, editors. Morphogenesis of Lung Cancer. Boca Raton, FL: CRC Press; 1982. p. 65-89.
[3] Kitamura H, Kameda Y, Ito T, Hayashi H. Atypical adenomatous hyperplasia of the lung. Am J Clin Pathol 1999;111:610-22.
[4] Boyse M, Yuan J. Cellular response to endoplasmic reticulum stress: a matter of life or death. Cell Death Differ 2006;13:363-73.
[5] Verkhratsky A. Physiology and pathophysiology of the calcium store in the endoplasmic reticulum of neurons. Physiol Rev 2005;85:201-79.
[6] Paschen W, Frandsen A. Endoplasmic reticulum dysfunction—a common denominator for cell injury in acute and degenerative diseases of the brain? J Neurochem 2001;79:719-25.
[7] Merad-Boudia M, Nicole A, Santiard-Baron D, Saille C, Ceballos-Picot I. Mitochondrial impairment as an early event in the process of apoptosis induced by glutathione depletion in neuronal cells: relevance to Parkinson's disease. Biochem Pharmacol 1998;56:645-55.
[8] Oyadomari S, Koizumi A, Takeda K, et al. Targeted disruption of the Chop gene delays endoplasmic reticulum stress–mediated diabetes. J Clin Invest 2002;109:525-32.
[9] Ito M, Jameson JL, Ito M. Molecular basis of autosomal dominant neurohypophyseal diabetes insipidus. Cellular toxicity caused by the accumulation of mutant vasopressin precursors within the endoplasmic reticulum. J Clin Invest 1997;99:1897-905.
[10] Ozcan U, Cao Q, Yilmaz E, et al. Endoplasmic reticulum stress links obesity, insulin action, and type 2 diabetes. Science 2004;306:457-61.
[11] Mori K. Tripartite management of unfolded proteins in the endoplasmic reticulum. Cell 2000;101:451-4.
[12] Patil C, Walter P. Intracellular signaling from the endoplasmic reticulum to the nucleus: the unfolded protein response in yeast and mammals. Curr Opin Cell Biol 2001;13:349-55.
[13] Parker R, Phan T, Baumeister P, et al. Identification of TFII-I as the endoplasmic reticulum stress response element binding factor ERSF: its autoregulation by stress and interaction with ATF6. Mol Cell Biol 2001;21:3220-33.
[14] Yoshida H, Okada T, Haze K, et al. Endoplasmic reticulum stress–induced formation of transcription factor complex ERSF including NF-Y (CBF) and activating transcription factors 6alpha and 6beta that activates the mammalian unfolded protein response. Mol Cell Biol 2001;21:1239-48.
[15] Haze K, Yoshida H, Yanagi H, Yura T, Mori K. Mammalian transcription factor ATF6 is synthesized as a transmembrane protein and activated by proteolysis in response to endoplasmic reticulum stress. Mol Biol Cell 1999;10:3787-99.
[16] Yoshida H, Matsui T, Yamamoto A, Okada T, Mori K. XBP1 mRNA is induced by ATF6 and spliced by IRE1 in response to ER stress to produce a highly active transcription factor. Cell 2001;107:881-91.
[17] Yoshida H, Haze K, Yanagi H, Yura T, Mori K. Identification of the cis-acting endoplasmic reticulum stress response element responsible for transcriptional induction of mammalian glucose–regulated proteins. Involvement of basic leucine zipper transcription factors. J Biol Chem 1998;273:33741-9.

[18] Ubeda M, Habener JF. CHOP gene expression in response to endoplasmic-reticular stress requires NFY interaction with different domains of a conserved DNA-binding element. Nucleic Acids Res 2000; 28:4987-97.
[19] Lee AS. GRP78 induction in cancer: therapeutic and prognostic implications. Cancer Res 2007;67:3496-9.
[20] Liu G, Pei F, Yang F, et al. Role of autophagy and apoptosis in non–small-cell lung cancer. Int J Mol Sci 2017;18:e367.
[21] Kim KM, Yu TK, Chu HH, et al. Expression of ER stress and autophagy-related molecules in human non–small cell lung cancer and premalignant lesions. Int J Cancer 2012;131:E362-70.
[22] Tsai HY, Yang YF, Wu AT, et al. Endoplasmic reticulum ribosome-binding protein 1 (RRBP1) overexpression is frequently found in lung cancer patients and alleviates intracellular stress-induced apoptosis through the enhancement of GRP78. Oncogene 2013;32: 4921-31.
[23] Deny MA, Jodom J, Ursini-Siegel J, et al. Endoplasmic reticulum stress induces PRNP prion protein gene expression in breast cancer. Breast Cancer Res 2013;15:R22.
[24] Kwon D, Koh J, Kim S, et al. Overexpression of endoplasmic reticulum stress–related proteins, XBP1s and GRP78, predicts poor prognosis in pulmonary adenocarcinoma. Lung Cancer 2018;122:131-7.
[25] Nakanishi K, Kawai T, Kumaki F, et al. Expression of mRNAs for telomeric repeat binding factor (TRF)-1 and TRF2 in atypical adenomatous hyperplasia and adenocarcinoma of the lung. Clin Cancer Res 2003;9:1105-11.
[26] Koga T, Hashimoto S, Sugio K, et al. Lung adenocarcinoma with bronchioloalveolar carcinoma component is frequently associated with foci of high-grade atypical adenomatous hyperplasia. Am J Clin Pathol 2002;117:464-70.
[27] Nakanishi K, Kawai T, Kumaki F, Hirot S, Mukai M, Ikeda E. Expression of human telomerase RNA component and telomerase reverse transcriptase mRNA in atypical adenomatous hyperplasia of the lung. Hum Pathol 2002;33:697-702.